AIP | Journal of Applied Physics

Negative differential resistance in electron tunneling in ultrathin films near the two-dimensional limit

R. Batabyal, A. H. M. Abdul Wasey, J. C. Mahato, Debolina Das, A. Roy et al.

Citation: J. Appl. Phys. **113**, 034308 (2013); doi: 10.1063/1.4775816
View online: http://dx.doi.org/10.1063/1.4775816
View Table of Contents: http://jap.aip.org/resource/1/JAPIAU/v113/i3
Published by the American Institute of Physics.

Related Articles

Simultaneous measurement of tunneling current and atomic dipole moment on Si(111)-(7×7) surface by noncontact scanning nonlinear dielectric microscopy
J. Appl. Phys. 113, 014307 (2013)

Dissipative transport in rough edge graphene nanoribbon tunnel transistors
Appl. Phys. Lett. 101, 263501 (2012)

Tunnel conductance in GaN:Mn/AlN/GaN:Mn (0001) junction from first-principles calculations
J. Appl. Phys. 112, 123711 (2012)

Response to "Comment on 'Zener tunneling semiconducting nanotubes and graphene nanoribbon p-n junctions'" [Appl. Phys. Lett. 101, 256103 (2012)]
Appl. Phys. Lett. 101, 256104 (2012)

Comment on "Zener tunneling in semiconducting nanotubes and graphene nanoribbon p-n junctions" [Appl. Phys. Lett. 93, 112106 (2008)]
Appl. Phys. Lett. 101, 256103 (2012)

Additional information on J. Appl. Phys.

Journal Homepage: http://jap.aip.org/
Journal Information: http://jap.aip.org/about/about_the_journal
Top downloads: http://jap.aip.org/features/most_downloaded
Information for Authors: http://jap.aip.org/authors

ADVERTISEMENT

AIP Advances
Now Indexed in Thomson Reuters Databases
Explore AIP's open access journal:
• Rapid publication
• Article-level metrics
• Post-publication rating and commenting

Downloaded 18 Jan 2013 to 14.139.222.34. Redistribution subject to AIP license or copyright; see http://jap.aip.org/about/rights_and_permissions

JOURNAL OF APPLIED PHYSICS **113**, 034308 (2013)

Negative differential resistance in electron tunneling in ultrathin films near the two-dimensional limit

R. Batabyal, A. H. M. Abdul Wasey, J. C. Mahato, Debolina Das, A. Roy,[a)] G. P. Das, and B. N. Dev[b)]
Department of Materials Science, Indian Association for the Cultivation of Science, 2A and 2B Raja S. C. Mullick Road, Jadavpur, Kolkata 700032, India

(Received 12 April 2012; accepted 26 December 2012; published online 17 January 2013)

We report on our observation of negative differential resistance (NDR) in electron tunneling conductance in atomic-scale ultrathin Ag films on Si(111) substrates. NDR was observed by scanning tunneling spectroscopy measurements. The tunneling conductance depends on the electronic local density of states (LDOS) of the sample. We show that the sample bias voltage, at which negative differential resistance and peak negative conductance occur, depends on the film thickness. This can be understood from the variation in the LDOS of the Ag films as a function of film thickness down to the two-dimensional limit of one atomic layer. First principles density functional theory calculations have been used to explain the results. © *2013 American Institute of Physics*. [http://dx.doi.org/10.1063/1.4775816]

I. INTRODUCTION

Atomic-scale thin films show interesting behavior in various properties. For example, thin magnetic films over a few atomic layers show unusual scaling behavior in Curie temperature[1] and interesting cross-over effect in magnetic domain orientation.[2] Superconductivity in ultrathin films of two-to-five atomic layer thickness has shown interesting variation in superconducting gap and transition temperature, the thinnest film being influenced by the proximity to the substrate.[3] Negative differential resistance (NDR), i.e., decreasing current with increasing voltage, was first observed in a tunnel diode by Esaki in 1958.[4] Since then, extensive experimental and theoretical research has led to applications of NDR in semiconductor devices which are used in modern electronics.[5–7] Here we investigate NDR, in atomic-scale ultrathin films. This would provide insight into electron transport phenomena in such films. The decrease in charge transport in spite of increasing driving force and its dimensional dependence can open up a new horizon in not only the fundamental aspects of electron transport in two-dimensional systems but also in the future of devices in reduced dimensionality. Scanning tunneling microscopy (STM), in conjunction with scanning tunneling spectroscopy (STS), allows us to explore transport mechanism in atomic-scale thin films. In STS, the origin of NDR is assigned, in general, to the alignment and misalignment of narrow features of both the tip and the sample electronic density of states (DOS) as the sample bias is swept.[8–12] The current can decrease if two narrow features in the sample DOS and the tip DOS move away from alignment. If the tip has featureless DOS, we would not observe NDR. In reality, the density of states of the tip can harbor narrow features. This has been recognized in STM studies of surfaces[9] and has been used to explain NDR in boron-doped silicon surfaces.[8] Sharp features in the tip DOS may appear at the tip apex atom if the tip is sufficiently sharp[10,11] or it has adsorbed atoms. In atomic-scale thin films, the electronic DOS is governed by the film thickness. The energy at which specific features (peaks) in DOS appear, shift with film thickness.[3,13] This thickness dependence of sample DOS plays a crucial role in controlling the NDR onset voltage.

Here, we describe the observation of NDR and the effect of film thickness in atomic-scale thin films, for the first time, using STS at room temperature (RT). The STS investigations were carried out on prototypical Ag ultrathin films on a Si(111) substrate, which is a nonreactive metal-semiconductor system. We show how the bias voltage at which NDR occurs depends on the thickness of the film, as the DOS of the thin films evolve with thickness. The results are explained semi-quantitatively on the basis of first-principles density functional theory (DFT) calculations.

II. EXPERIMENTAL

The experiments were performed using a compact molecular beam epitaxy (MBE) system with an attached variable temperature scanning tunneling microscope (VT-STM) [Omicron Nanotechnology], operating under ultrahigh vacuum (UHV) condition. The base pressure in both the MBE and the STM chamber was less than 1.0×10^{-10} mbar. Ag thin films were grown on atomically clean Si(111)-(7×7) surfaces. N-type Si(111) substrates were degassed at 600 °C for 15 h and flashed at ∼1200 °C for a minute to obtain clean 7×7 reconstructed surfaces. The growth of Ag on Si(111)-7×7 surfaces is achieved by depositing Ag atoms onto the substrates at RT, from a Knudsen cell maintained at 920 °C. Initially, we observed the reconstructed Si(111)-(7×7) surface and the morphology of the Ag films using a clean W tip in scanning tunneling microscopy (STM). Tunneling current (I) was measured as a function of sample bias voltage (V) using this W tip. These I-V curves did not show any NDR. When

a)Present address: Microelectronics Research Center, J. J. Pickle Research Campus, The University of Texas at Austin, Texas 78758, USA.
b)Email: msbnd@iacs.res.in.

 © 2013 American Institute of Physics

Downloaded 18 Jan 2013 to 14.139.222.34. Redistribution subject to AIP license or copyright; see http://jap.aip.org/about/rights_and_permissions

the DOS of the tip has no sharp feature, NDR is not expected to be observed, even though the sample may have features suitable for displaying NDR. It is necessary to prepare a tip with sharp features in DOS in order to observe NDR. We crashed the W tip onto the Ag film which presumably modified the tip apex by adsorbing a cluster of Ag atoms (or a single Ag atom) at the tip apex. Considering the fact that Ag has a much smaller surface free energy (1.30 Jm^{-2}) compared to W (3.47 Jm^{-2}),[14] Ag would wet the W surface. From this wetting condition, it expected that some Ag atoms would be collected on the W tip when it is crashed onto a Ag film. STS measurements were carried out using the modified tip. These measurements have shown NDR. A 2-monolayer (2ML) Ag film was deposited on a Si(111)-(7 × 7) substrate. [Here 1 ML of Ag is equivalent to the nominal surface atomic density of Ag(111), 1.5×10^{15} atoms/cm^2, as in Refs. 15 and 16]. This has produced flat-top islands of different heights. As observed earlier,[16] Ag islands of various heights can be obtained in a single deposition, although there is a preference for certain heights. STS measurements were carried out on height-selected islands for the investigation of film thickness dependence of NDR. *I-V* measurements were made at voltage steps of 0.08 V.

III. RESULTS AND DISCUSSIONS

Fig. 1(a) shows a typical constant current STM topographical image taken on the 2 ML Ag-deposited film on a Si(111) surface at RT. Fig. 1(b) shows the height distribution from a selected area of the image in Fig. 1(a). The peak at 0.0 corresponds to the wetting layer [1 atomic layer (AL) Ag]. Fig. 1(b) shows the preference for islands of heights containing an even number of atomic layers on top of the wetting layer as observed earlier.[16] However, islands containing an odd number of atomic layers on top of the wetting layer are also observed, albeit with less abundance. Fig. 1(c) shows two height profiles along two lines marked on Fig. 1(a). The height profiles show heights of 2-AL, 3-AL, 4-AL, and 5-AL on Si. Point "1" marked on Fig. 1(a) is on the wetting layer (1-AL). We performed STS measurements selectively on the positions marked by circles and numbers "1"-"5" (see Fig. 1) which correspond to the islands of different thicknesses. A standard W tip, which is used for usual STM and STS experiments, has a relatively flat DOS and is not suitable for observing NDR. As seen in Fig. 2 top panel, no NDR is observed with a standard W tip. The presence of sharp features in the DOS of the tip is necessary to observe NDR in tunneling experiments. As mentioned earlier, sharp features in the tip DOS may appear at the tip apex atom if the tip is sharp or it has adsorbed atoms and such tips have been used to observe NDR.[10,11] We have modified a standard W tip by crashing it onto one part of the Ag film. With this modified tip, we have observed NDR. The tip apparently gets modified by being sharper or by adsorbing Ag atom(s), essentially producing sharp electronic states at the tip. The plots of tunneling current (I) versus sample bias voltage (V), measured with the modified W tip on those marked islands, are shown in Fig. 2 and designated by the numbers accordingly. The *I-V* curves show NDR effect at a negative bias

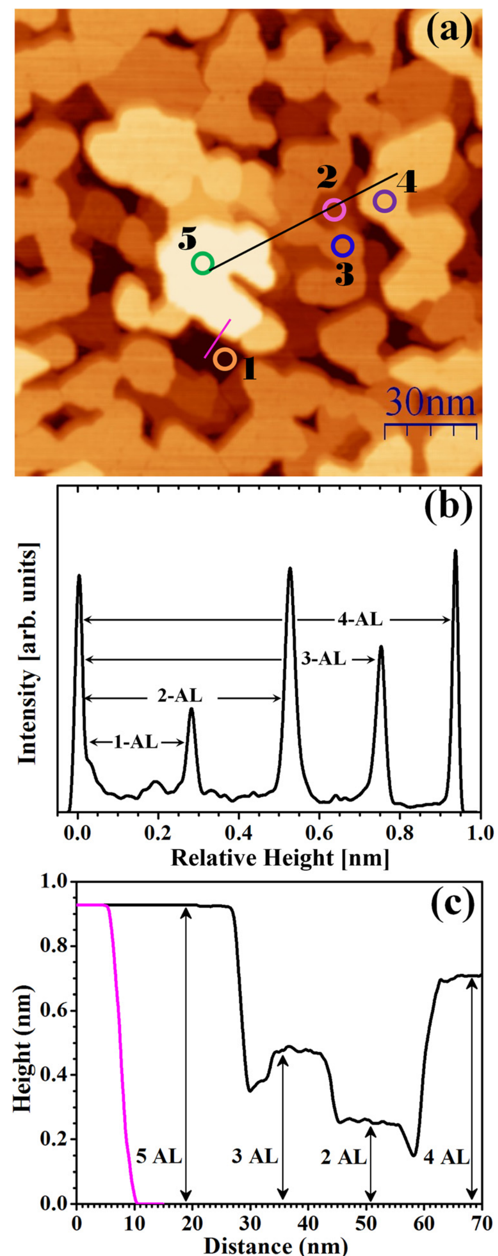

FIG. 1. (a) A constant current STM topograph of a Ag thin film on a Si(111)-7 × 7 surface. STS measurements were made on the spots, marked by circles (also marked by numbers), which are of different thicknesses; (b) A selected area height distribution of the Ag islands in (a). The peak at 0.0 nm corresponds to the wetting layer. The peak between 0.9 and 1.0 nm corresponds to a 4-AL thick film on the wetting layer; (c) Line profiles of the islands marked in (a) with corresponding colors. The thickness at spot "5" is 4-AL on the wetting layer (i.e., 5-AL on Si).

voltage. The black vertical lines in Fig. 2 indicate the voltages at which NDR starts (except for the case "2"). At those positions, negative tunneling conductance is observed. For the case "2," although not negative, a minimum in the tunneling conductance is observed. As the film thickness increases, the *I-V* characteristics depict a clear shift of the NDR onset voltage towards more negative bias voltages. For reference, a *I-V* curve for a 5-AL film, obtained by using an unmodified tip, is shown in the topmost panel. This does not show any NDR. The *I–V* curves for the other cases, obtained with an unmodified tip, also do not show NDR.

Downloaded 18 Jan 2013 to 14.139.222.34. Redistribution subject to AIP license or copyright; see http://jap.aip.org/about/rights_and_permissions

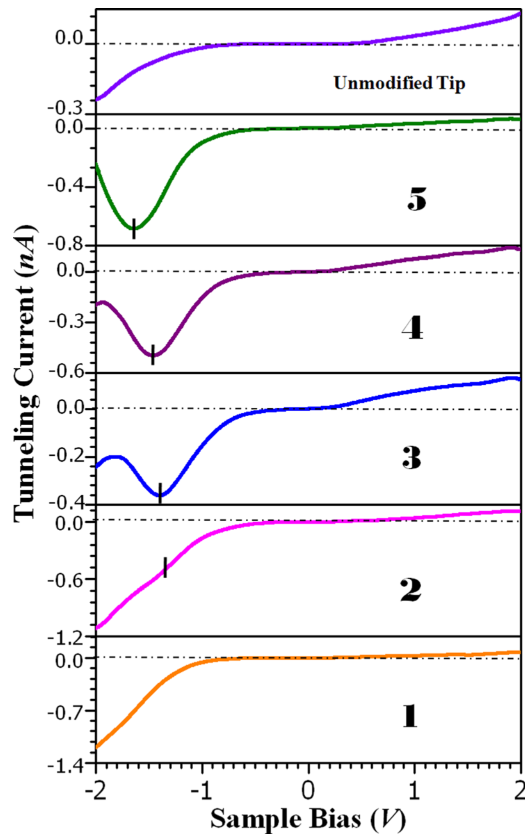

FIG. 2. Tunneling current (I) vs. sample bias voltage (V) characteristics at the marked positions in Fig. 1. The vertical black marks indicate the NDR onset voltages. In the topmost panel, an I-V curve, obtained with a clean unmodified W tip on a 5-AL height island on Si, is shown. This does not show NDR.

The numerical derivative [dI/dV] of the I-V data, obtained from STS, is proportional to the tunneling conductance of the system dV/dI is the differential resistance (DR). Fig. 3(a) shows the tunneling conductance versus sample bias voltage (the color code of the curves corresponds to that in Fig. 2) and explicitly confirms the presence of NDR effect at negative bias voltages. A close look at the tunneling conductance data reveals that from zero bias to the negative bias, tunneling conductance increases as usual and reaches a maximum and then the conductance tends to decrease. For islands of higher thicknesses, such as those marked "3," "4," and "5" in Fig. 1, the conductance goes to negative values and reaches a minimum. Whereas, for the island of lower thickness marked by "2" in Fig. 1, the conductance, after passing through a maximum, drops to a lower positive conductance minimum, without ever going to negative. For the island marked "1," also zero or negative conductance is not observed. The arrows in Fig. 3(a) indicate the positions of the conductance minima.

Significantly, all the STS data except those on island "1" and "2," reveal the NDR on the valence band side. The highest amount of negative differential conductance (NDC) is observed for the island "5." As the island thickness decreases, the amount of NDC decreases as well. In Fig. 3(b), we present the voltage at which the tunneling conductance shows a minimum in the NDR region (indicated by red arrows in Fig. 3(a)) with the thickness of the islands. The conductance for island "2" shows a minimum but no NDR.

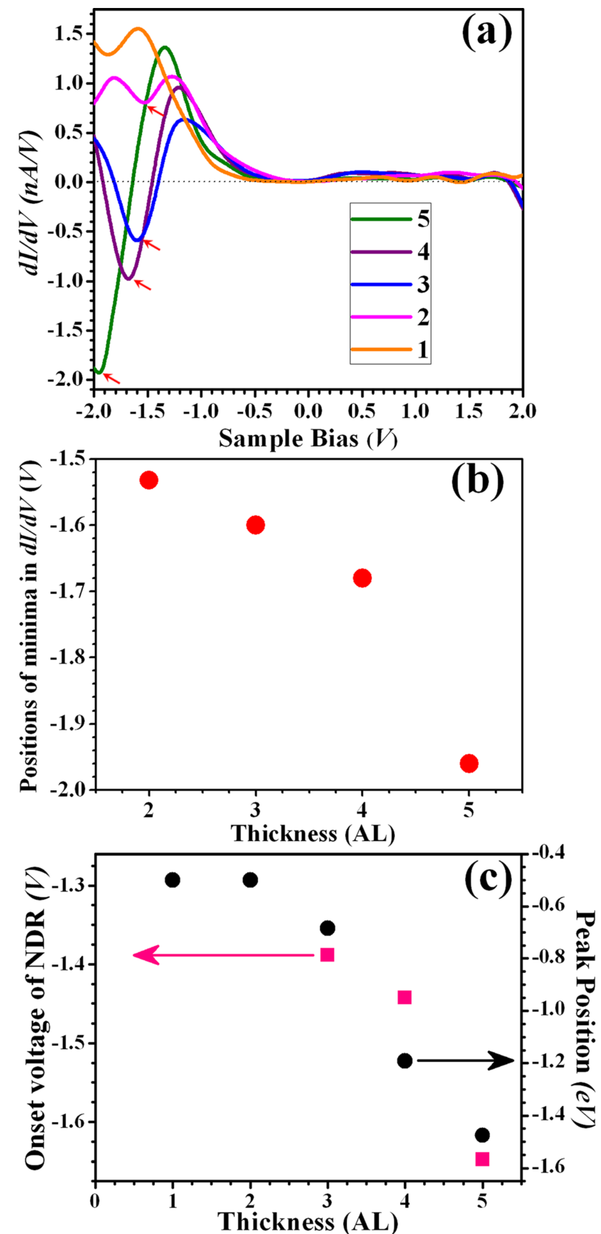

FIG. 3. (a) Tunneling conductance (dI/dV) vs. sample bias (V) voltage plot, obtained by numerical derivatives of the I-V data, clearly shows the NDR effect; (b) positions of minima in tunnelling conductance in (a), marked by red arrows, are shown as a function of film thickness; (c) NDR onset voltages and peak positions in Fig. 5(a), calculated from DFT, are plotted with the film thickness.

Fig. 3(b) clearly shows that this voltage gradually shifts to a more negative value as the thickness of the film increases. Fig. 3(c) shows the NDR onset voltage along with the DFT results of a peak position shift as a function of film thickness. DFT results are described latter.

Fig. 4 shows a schematic band diagram for explaining the NDR in the present context. Figs. 4(a)–4(c) show tip local density of states (LDOS) on the right side and sample LDOS on the left side. In Fig. 4(a), there is no sample bias ($V=0$) and the Fermi levels of the sample and the tip coincide, preventing the electrons from tunneling. In Fig. 4(b)), a negative bias ($-V_1$) is applied to the sample. This leads to the lowering of the Fermi level of the tip and eventually the tunneling of electrons from sample to tip occurs.[17] Due to the sharp

Downloaded 18 Jan 2013 to 14.139.222.34. Redistribution subject to AIP license or copyright; see http://jap.aip.org/about/rights_and_permissions

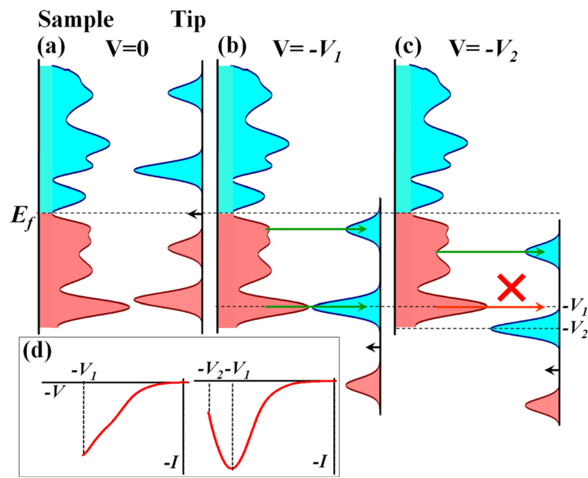

FIG. 4. The tunneling mechanism for NDR is schematically shown for the negative sample bias voltages. (a), (b), and (c) show the sample-tip LDOS near the Fermi energy with different bias voltages; (d) corresponding *I-V* characteristics for situations (b) and (c) are schematically shown.

features in LDOS at the tip apex, as we go on increasing negative sample bias, there is a condition when filled sample states find no empty tip states at the same energy level for electrons to tunnel into. Fig. 4(c) depicts such a condition where sample bias is $-V_2$; tip Fermi level is further lowered and consequently tunneling is no more possible for the lower energy state, although it is possible for the higher energy state. In Fig. 4(d), the corresponding *I-V* characteristics have been shown. For sample bias upto $-V_1$, empty states for tunneling are available at the same energy, leading to the continuous increase of current. However, in the region of the sample bias between $-V_1$ and $-V_2$, tip empty states at the same energy are less available; this leads to an appreciable drop of tunneling current.

As the DOS feature on the W tip remains the same for all measurements, the change in NDR phenomena, namely the onset voltage of NDR and the position of the peak conductance, can be attributed to the change in sample DOS due to the Ag layer thickness. We have performed first principles DFT calculations[18,19] to investigate the dependence of LDOS on film thickness for ultrathin Ag films on Si(111) surfaces. For DFT calculations, we have used the code *Vienna Ab Initio Simulation Package* (VASP).[20] Projector augmented wave (PAW)[21] potentials were employed for elemental constituents, viz., Ag, W, and Si potentials. Generalized gradient approximation (GGA) functional of Perdew, Burke, and Ernzerhof (PBE) has been used[22] for calculating the exchange-correlation energy. Brillouin zone sampling has been done using Monkhorst-Pack[23] method using $2 \times 2 \times 1$ **k**-mesh. For all the calculations, self-consistency has been achieved with a 0.1 meV convergence in total energy. Cut off energy of 400 eV for the plane wave basis has been used. To obtain the optimized ground state geometry, "forces" have been converged to less than 0.01 eV/Å by conjugate gradient minimization.[24,25] We first construct the model of Ag(111) layers on a Si(111) substrate (see the inset of Fig. 5(b)). If we make a heterojunction between Ag(111) and Si(111) planes, the resulting lattice mismatch will be ~25%. However, coincidence site lattice matching between a 4×4 unit cell of Ag and a 3×3 unit cell of Si reduces the

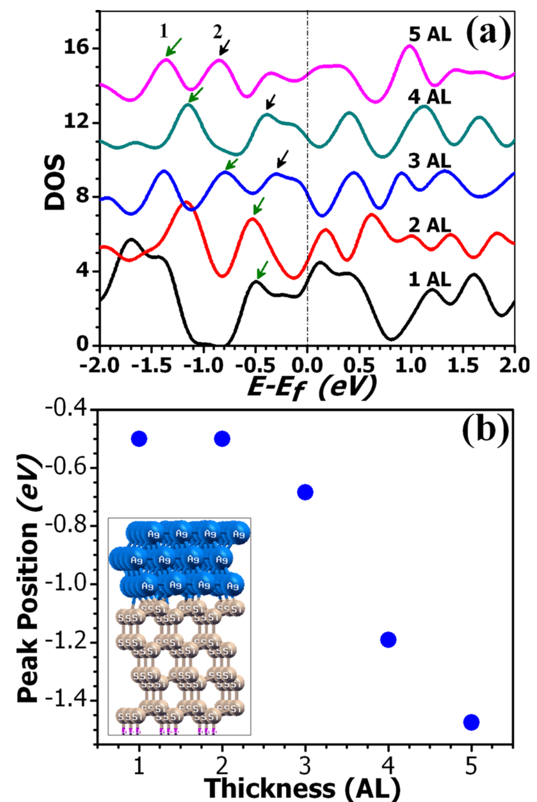

FIG. 5. (a) Electronic DOS for Ag thin films of different thicknesses (1-5 atomic layers), as obtained from DFT calculations. Green and black arrows show the corresponding shift of peak position. (b) Peak position vs. thickness plot of the particular energy state marked by green arrows in (a). Theoretical model for DFT calculation representing the sample ground state geometry [for 3-AL Ag on Si(111)] is shown in the inset of (b).

lattice mismatch to ~0.31%, which makes epitaxial growth of Ag on Si possible.[26,27] Thus every fifth atom of Ag is sitting above exactly on the fourth atom of Si. So we have designed a theoretical model of the Ag/Si(111) system for DFT study forming Ag atoms in a (4×4) cell and placing it on a (3×3) cell of the Si(111) surface to form a Ag(111) layer. We have taken four bilayers of Si(111) to make a Si(111) slab in order to represent the substrate when the other side of the Si(111) slab has been passivated with hydrogen atoms to saturate the dangling bond states of Si(111) surface atoms. A single atomic layer of Ag(111) on four bilayers of Si(111) represents the wetting layer of the Ag/Si(111) system in the experimental study. Next, we have placed more number of Ag(111) layers on Si(111) for studying electronic structures of Ag on Si(111) as a function of Ag layer thickness. Fig. 5 shows the results of our DFT calculations. The inset in Fig. 5(b) shows the geometrically optimized structures of the sample with three atomic layers of Ag. Fig. 5(a) shows the LDOS of the topmost Ag layer for 1-AL, 2-AL, 3-AL, 4-AL, and 5-AL Ag films. This has been obtained from the layer projected density of states of Ag thin films of various thicknesses. Integrated LDOS for all Ag layers plus four Si layers show similar features. For the 1-AL and 2-AL films, there are some contributions in the LDOS from the p-states of the substrate Si. LDOS clearly show the shift of the energy position with film thickness for individual states below the Fermi energy (marked by green and black

Downloaded 18 Jan 2013 to 14.139.222.34. Redistribution subject to AIP license or copyright; see http://jap.aip.org/about/rights_and_permissions

arrows). In Fig. 5(b), the shifting of the energy of a state (marked by green arrow in Fig. 5(a)) with the film thickness of the Ag layer is shown. These values are also shown in Fig. 3(c) along with the experimental results. The shift of the energy of the states deeper into the valence band with increasing film thickness leads to the shifting of the onset voltage in the NDR regime. This can be easily understood from the schematic in Fig. 4 by shifting the sample LDOS below E_f further down as in the theoretical LDOS. DFT calculations show a shift of peak position of LDOS towards higher negative voltage (i.e., towards lower energy) with increasing island height. As a consequence, NDR transition occurs at higher negative voltages as island thickness increases. Such shift in peak positions in DOS towards lower energy for higher film thickness has also been observed in exploring superconductivity near the two-dimensional limit.[3] In these investigations, superconducting transition temperature and energy gap have been found to depend on the (Pb) film thickness over 2AL–5AL range.[3] The authors observed that for the 2-AL film (the thinnest investigated) Cooper pair binding energy is strongly affected by the substrate. Our DFT calculation also shows that LDOS across the Ag/Si interface are strongly affected upto a couple of atomic layers of Ag and Si from the interface. Interestingly, these Si layers near the interface do not have band gap due to the presence of metal induced gap states within the gap. These details will be published elsewhere.[27] That the peak "1" ("2") in Fig. 5(a) marked by green arrows (marked by black arrows) is indeed the same peak shifted in energy for change in film thickness has been confirmed by analyzing the character of these peaks. The ratio of Ag *d* to *s* contribution in peak "1" is $\geq$1.5 and that in peak "2" is $\sim$1. These values are different for 1-AL and 2-AL cases, where the DOS is affected by underlying Si, and also the peak "2" is in the conduction band. These ratios are obtained from the site- and angular momentum projected density of states.

It is noticed from Fig. 3(c) that the trend of NDR onset voltage and the sample LDOS peak position as a function of film thickness agree well. However, there is an offset of the voltage between theory and experiment. This NDR onset voltage depends on the peak positions in the DOS of the tip as seen from the illustration in Fig. 4. For a full quantitative agreement, one needs to know the DOS of the tip precisely. We have carried out a DFT calculation assuming a capture of ten Ag atoms at the W tip. We optimized the geometry of this tip and obtained the tip DOS. Near the Fermi level, the DOS shows sharp peaks at 0.1 eV, 0.4 eV and at higher energies in the conduction band and at -0.4 eV, -0.7 eV and at lower energies in the valence band. While this has helped us in making the illustrations in Fig. 4, this cannot be used for a quantitative comparison. The peak positions in the tip DOS would depend on the number of adsorbed Ag atoms and the consequent optimum geometry of the tip, or on the structure of the W tip in case no Ag atoms are adsorbed and only the W tip has been sharpened. Without the precise knowledge about the tip, it is practically impossible to obtain a full quantitative agreement between theory and experiment. However, the semi-quantitative agreement between theory and experiment provides an understanding of the physics of dependence of NDR onset voltage on the film thickness in ultrathin films near the two-dimensional limit.

IV. CONCLUSIONS

We have investigated the negative differential resistance (NDR) behavior in atomic-scale thin films near the two-dimensional limit of one atomic layer. As an example, we have used Ag on Si(111) surfaces for scanning tunneling spectroscopy experiments. The sample bias voltage at which the NDR sets in has been found to depend on the film thickness. The results have been semi-quantitatively explained by density functional theory calculations. The observed variation of the NDR onset voltage has been attributed to the changes in the electronic density of states (DOS) in the valence band near the Fermi level. We believe such NDR behavior would be observed in other systems. For one- and two-atomic layer films no NDR was observed. Electronic structures in these films are influenced by the substrate. Our DFT calculation for the Ag/Si(111) system, not only shows the influence of the substrate on Ag layers near the interface, but also the influence of Ag on the Si substrate. Layer projected DOS reveal that up to the third atomic layer of Si from the interface, metal induced gap states (MIGS) remove the usual band gap of semiconducting Si. An experiment on Si layers deposited on a Ag substrate would reveal this feature. The dependence of NDR on film thickness in ultrathin films, as presented here, may be useful in designing novel electronic devices using two-dimensional layers.

ACKNOWLEDGMENTS

Jagadish C. Mahato and Debolina Das are supported by CSIR Fellowship 09/080 (0674)/2009-EMR-I and 09/080 (0725)/2010-EMR-I respectively. A. H. M. Abdul Wasey is supported by the IBIQuS project. The work is partially supported by the IBIQuS project. We acknowledge the help provided by S. Naskar in the laboratory.

[1] R. Zhang and R. F. Willis, Phys. Rev. Lett. **86**, 2665 (2001).
[2] R. Allenspach, M. Stampanoni, and A. Bischof, Phys. Rev. Lett. **65**, 3344 (1990).
[3] S. Qin, J. Kim, Q. Niu, and C.-K. Shih, Science **324**, 1314 (2009).
[4] L. Esaki, Phys. Rev. **109**, 603 (1958).
[5] J. R. Soderstrom, E. R. Brown, C. D. Parker, L. J. Mahoney, J. Y. Yao, T. G. Andersson, and T. C. McGill, Appl. Phys. Lett. **58**, 275 (1991).
[6] R. H. Mathews, J. P. Sage, T. C. L. G. Sollner, S. D. Calawa, C.-L. Chen, L. J. Mahoney, P. A. Maki, and K. M. Molvar, Proc. IEEE **87**, 596 (1999).
[7] T. P. E. Broekaert, B. Brar, J. P. A. van der Wagt, A. C. Seabaugh, F. J. Morris, T. S. Moise, E. A. Beam, and G. A. Frazier, IEEE J. Solid State Circ. **33**, 1342 (1998).
[8] I.-W. Lyo and Ph. Avouris, Science **245**, 1369 (1989).
[9] R. Wiesendanger and H.-J. Guntherodt, *Scanning Tunneling Microscopy III* (Springer-Verlag, Berlin, 1993).
[10] A. L. Yeyati, A. Martín-Rodero, and F. Flores, Phys. Rev. B **56**, 10369 (1997).
[11] S. Datta, W. Tian, S. Hong, R. Reifenberger, J. I. Henderson, and C. P. Kubiak, Phys. Rev. Lett. **79**, 2530 (1997).
[12] Y. Xue, S. Datta, S. Hong, R. Reifenberger, J. I. Henderson, and C. P. Kubiak, Phys. Rev. B **59**, 7852 (1999).
[13] J. Kim, S. Qin, W. Yao, Q. Niu, M. Y. Chou, and C-K. Shih, Proc. Natl. Acad. Sci. USA **107**, 12761 (2010).
[14] L. Z. Mezey and J. Giber, Jpn. J. Appl. Phys. **21**, 1569 (1982).

Downloaded 18 Jan 2013 to 14.139.222.34. Redistribution subject to AIP license or copyright; see http://jap.aip.org/about/rights_and_permissions

[15]L. Gavioli, K. R. Kimberlin, M. C. Tringides, J. F. Wendelken, and Z. Zhang, Phys. Rev. Lett. **82**, 129 (1999).
[16]D. K. Goswami, K. Bhattacharjee, B. Satpati, S. Roy, P. V. Satyam, and B. N. Dev, Surf. Sci. **601**, 603 (2007).
[17]Supriyo Datta, *Electronic Transport in Mesoscopic Systems* (Cambridge University Press, Cambridge, 1995).
[18]P. Hohenberg and W. Khon, Phys. Rev. **136**, B864 (1964).
[19]W. Kohn and L. Sham, Phys. Rev. **140**, A1133 (1965).
[20]G. Kresse and J. Hafner, Phys. Rev. B **47**, 558 (1993).
[21]P. E. Blöchl Phys. Rev. B **50**, 17953 (1994).
[22]J. Perdew, K. Burke, and M. Ernzerhof Phys. Rev. Lett. **77**, 3865 (1996).
[23]H. J. Monkhorst and J. D. Pack Phys. Rev. B **13**, 5188 (1976).
[24]W. H. Press, B. P. Flannery, S. A. Tenkolsky, and W. T. Vetterling, *Numerical Recipes*, (Cambridge University Press, New York, 1986), Vol. 1.
[25]P. Pulay Chem. Phys. Lett. **73**, 393 (1980).
[26]G. N. Kakazei, P. P. Martin, A. Ruiz, M. Varela, M. Alonso, E. Paz, F. J. Palomares, F. Cebollada, R. M. Rubinger, M. C. Carmo, and N. A. Sobolev, J. Appl. Phys. **103**, 07B527 (2008).
[27]A. H. M. Abdul Wasey, R. Batabyal, J. C. Mahato, B. N. Dev, Y. Kawazoe, and G. P. Das, Phys. Status Solidi B, 1–7 (2012).

Downloaded 18 Jan 2013 to 14.139.222.34. Redistribution subject to AIP license or copyright; see http://jap.aip.org/about/rights_and_permissions